First-principles study of the intrinsic defects in PbFCl

Bo Liu,[1,*] Zeming Qi,[2] and Chaoshu Shi[1,2]
[1]*Department of Physics, University of Science and Technology of China Hefei, 230026, China*
[2]*NSRL, University of Science and Technology of China Hefei, 230027, China*
(Received 4 April 2006; revised manuscript received 14 August 2006; published 1 November 2006)

First-principles pseudopotential calculations have been performed to investigate intrinsic defects including vacancies, interstitials, antisite defects, as well as Schottky and Frenkel defects in PbFCl crystals. For the isolated vacancies and interstitials, their formation energies are critically dependent on the atomic chemical potentials and electron Fermi energy. The charged defects for vacancies and interstitials are stable in a wide range of Fermi level, suggesting a strong ionization tendency. The present calculations also reveal that the formation energies of Schottky defects are much lower than those of Frenkel defects. Therefore it can be concluded that the Schottky defects are dominant in PbFCl crystals. Furthermore, Schottky defects ($V_{Pb}+V_F+V_{Cl}$) exhibit the lowest formation energy of 2.21 eV. Defect transition energy levels can occur between different charged states. The anion interstitials and the cation vacancies form acceptorlike defects with transition energies of 1.05, 0.57, and (0.47,0.9) eV for F_i, Cl_i and V_{Pb}, respectively, while V_F, V_{Cl}, and Pb_i have high transition energies of more than 3 eV. In addition, the calculated profiles of densities of states for the defective supercells show that some extra states may appear in the band gap.

DOI: 10.1103/PhysRevB.74.174101 PACS number(s): 71.20.−b, 74.62.Dh

I. INTRODUCTION

PbFCl crystals belong to the matlockite structure.[1] The matlockite structure with space group $P4/nmm$ (D_{4h}^7, no.129) is characterized by the tetragonal layered structure which consists of plans perpendicular to the c-axis. The Pb ions are on one side coordinated by a plane of four fluorine ions and on the other side coordinated by five Cl ions, of which one is on the c-axis out of the plane formed by the others, shown in Fig. 1. There are two PbFCl molecules per unit cell. The properties of other matlockite structure compounds MFX (M=Sr,Ba; X=Cl,Br) have been extensively investigated because of their practical applications. For example, BaFX(X=Cl,Br):Eu is a good x-ray phosphor for medical imaging[2,3] SrFCl:Sm can be used as sensor to measure the pressure in diamond anvil cells at high temperature[4,5] Recently, the investigation on PbFCl is attracting more attention because the potential application as scintillator has been found. High-quality PbFCl crystals were grown by a modified Bridgeman method at the Shanghai Institute of Ceramics, China[6,7] The scintillation light yield is about 20% that of the BGO scintillator at room temperature[8] A scintillation light with decay constants of 4 and 35 ns was obtained, a considerable luminescence intensity at room temperature, in contrast to previous reports.[9,10] The PbFCl single crystal is a promising scintillator to substitute lead perchlorate solution for a neutrino telescope to observe galactic supernovae due to many advantages.[8] Theoretical studies of the electronic properties of the matlockite structure compounds MFX (M=Sr,Ba,Pb, X=Cl,Br) can be found in the past few years[11,12] Kanchana *et al.* calculated the structural and electronic properties of SrFBr, SrFI, and CaFBr using the tight binding linear muffin-tin orbital (TB-LMTO) method.[11] Hassan *et al.* theoretically studied the electronic properties of MFX (M=Sr,Ba,Pb; X=Cl,Br,I) using the full-potential linearized augmented plane wave (FP-LAPW) method.[12] We have reported the electronic, optical, and luminescence properties in PbFCl using first-principles calculations and optical spectra experiments.[13]

It has been established that the defects in PbFCl can affect many properties on optical absorption, luminescence, thermoluminescence, and ion conductivity. For instance, the luminescent center for blue-violet emission in PbFCl may be related to the transition on Pb^{2+} ion in the presence of a defect center for blue-violet emission.[10] The ionic conductivity measurements showed that the ionic conduction in PbFCl may be caused by Schottky-type defects.[14–16] Islam calculated the formation energies for point defects and obtained the ion-transport mechanisms in PbFCl using an atomistic simulation technique,[17,18] indicating that the vacancies rather than interstitials are the dominant intrinsic defects and the Schottky-like disorder involving Pb and Cl vacancies are energetically favorable.

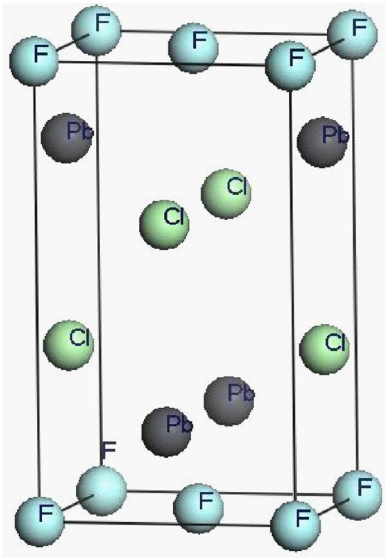

FIG. 1. (Color online) Crystal structure of PbFCl.

In the present work, the first-principles pseudopotential method was used to calculate the defect formation energies and electrical transition levels in PbFCl. We obtained the defect formation energies dependent on the chemical potentials and electron Fermi energy. These results yield important insight into the chemical environment effect on the defect formation energies. In contrast to Islam's constant formation energies independent of the chemical potentials and Fermi energy, the present work, therefore, provides more accurate and comprehensive information on the defects in PbFCl. The rest of this paper is organized as follows. In Sec. II, the calculational methods are described in detail. In Sec. III, we present the results and discussion including the defect formation energies for isolated point defects and electronic transition levels. Furthermore, the formation energies for Schottky and Frenkel defects are calculated and discussed. The density of states and contour plot of electronic charge density for perfect and defective supercells are also shown. Finally, we give a brief summary in Sec. IV.

II. METHOD OF CALCULATION

A. Details of the calculations

First-principles total-energy calculations of PbFCl were performed using the ABINIT code,[19,20] which is based on pseudopotentials and plane waves. It relies on an efficient fast Fourier transform algorithm[21] for the conversion of wave functions between real and reciprocal space on the adaptation to a fixed potential of the band-by-band conjugate gradient method[22] and on a potential-based conjugate-gradient algorithm for the determination of the self-consistent potential.[23] Exchange and correlation were treated in the generalized gradient approximation (GGA)[24] based on the density functional theory (DFT).[25] The pseudopotentials have been generated thanks to the FHI98PP code.[26] The electronic wave functions were expanded in plane waves up to a kinetic energy cutoff of 36 Ha (980 eV) to achieve convergence of total energies better than 1 meV/atom. A $4\times4\times4$ k-point grid based on the primitive vectors of the reciprocal space was applied. Firstly, we optimized the lattice constant for the unit cell (two PbFCl molecules) with the experimental lattice constants ($a=b=4.106$ Å, $c=7.23$ Å) as initial input. The calculated lattice constants ($a=b=4.143$ Å, $c=7.29$ Å) are very consistent with the experimental data. The 96-atom supercell with $4\times2\times2$ in the x,y,z directions obtained by repeating the optimized structure of the perfect unit cell was used in the defect calculations. Numerical integrations over the Brillouin zone were performed only at the Z point where the direct gap is located because of the large size of the supercell. To check the convergence, we used a larger $4\times3\times2$ 144-atom supercell to calculate the formation energy for vacancies (Pb and F). The estimated error of formation energy is less than 0.1 eV. Therefore, the 96-atom supercell is an appropriate choice for defect calculations. To introduce an isolated vacancy of Pb, F, and Cl, an interior atom was removed from the supercell. For interstitial cases, an atom was added to the supercell at the possible site. All the atoms in the defective supercell were allowed to relax using the Broyden-Fletcher-Goldfarb-Shanno (BFGS)[27] algorithm until the maximum residual force was less than 5 meV/Å.

B. Defect formation energies and transition energies

Based on the standard formalism by Zhang and Northrup,[28] the formation energy $\Delta H_f(\alpha,q)$ of a defect α in charge state q is a function of both the electron Fermi energy E_F and the chemical potentials of the species involved in the defect,

$$\Delta H_f(\alpha,q) = \Delta E(\alpha,q) + n_{\mathrm{F}}\mu_{\mathrm{F}} + n_{\mathrm{Cl}}\mu_{\mathrm{Cl}} + n_{\mathrm{Pb}}\mu_{\mathrm{Pb}} + qE_F, \tag{1}$$

where

$$\Delta E(\alpha,q) = E(\alpha,q) - E(perfect) + n_{\mathrm{F}}\mu_{\mathrm{F}}^0 + n_{\mathrm{Cl}}\mu_{\mathrm{Cl}}^0 + n_{\mathrm{Pb}}\mu_{\mathrm{Pb}}^0 + qE_{VBM}. \tag{2}$$

and where $E(\alpha,q)$ is the total energy of the supercell containing a defect in a charge state q. $E(perfect)$ is the total energy of the perfect supercell. For the studies of charged defects, an electron or two electrons are added or removed from the neutral system and a uniform background with opposite polarity is adopted automatically to keep the neutrality of the whole system, so the total energy per cell does not become infinite. The n's are the number of the corresponding atoms removed from the supercell to the reservoirs in forming the defect supercell. μ_{F}^0 and μ_{Cl}^0 were obtained from the calculated total energies of F_2 and Cl_2 molecules in a cubic box of $15\times15\times15$ Å^3, and μ_{Pb}^0 was obtained by calculating the total energy of ground-state solid Pb (fcc). μ_i is the chemical potential of constituent i relative to its chemical potential μ_i^0 in elemental phase. E_{VBM} is the energy of valence-band maximum. However, E_{VBM} in defective supercells is generally different from the one in perfect supercells due to the fact that the defect causes significant distortion to the band structure around the band gap. In order to determine E_{VBM} of the defective supercell, the band structures of perfect and defective supercells must be lined up[29] E_F is the Fermi energy of the electrons referenced to the valence band maximum of PbFCl.

The calculated band gap (3.5 eV) is much smaller than the experimental value (5.2 eV),[13] which is a commonly observed feature of GGA calculation. The difference ($\Delta E_{gap}=1.7$ eV) can affect the formation energy so that the correction is needed. The conduction band is shifted upward by ΔE_{gap} to match the experimental gap. Due to the underestimated CBM, the defect formation energy should be corrected by adding a value of $n\times\Delta E_{gap}$ for donorlike defects, where n is the number of the electrons at the defect. For instance, 1×1.7 eV is added to the formation energy of V_{F}^0. No correction is needed for the acceptorlike defects.

The defect transition energy level $\varepsilon_\alpha(q/q')$ is defined as the value of the Fermi level where the formation energy of q is equal to that of another charge q' of the same defect, i.e.,[30]

$$\varepsilon_\alpha(q/q') = [\Delta E(\alpha,q) - \Delta E(\alpha,q')]/(q'-q). \tag{3}$$

TABLE I. Formation free energies (in eV) for PbF_2, $PbCl_2$, and PbFCl.

Constituents	This work calculated data	Experimental data
$Pb+F_2 \rightarrow PbF_2$	−7.11	−7.01[a]
$Pb+Cl_2 \rightarrow PbCl_2$	−3.58	−3.72[a]
$Pb+\frac{1}{2}F_2+\frac{1}{2}Cl_2 \rightarrow PbFCl$	−5.46	−5.54[b]

[a]Reference 33.
[b]Reference 34.

C. Limits on atomic chemical potentials

We establish the ranges of chemical potentials for the constituent elements. The chemical potentials are restricted by the following equilibrium conditions:

$$\mu_{Pb} + \mu_F + \mu_{Cl} = \Delta H_f(PbFCl) \quad (4)$$

is the equilibrium condition for formation of PbFCl.

$$\mu_{Pb} + 2\mu_F \leq \Delta H_f(PbF_2), \quad (5)$$

$$\mu_{Pb} + 2\mu_{Cl} \leq \Delta H_f(PbCl_2) \quad (6)$$

are required to prevent the formation of PbF_2 and $PbCl_2$, respectively.

$$\mu_{Pb} \leq 0, \quad \mu_F \leq 0, \quad \mu_{Cl} \leq 0 \quad (7)$$

is also needed to prevent precipitation of elemental solid (Pb) or molecule (F_2 and Cl_2), respectively, where ΔH_f is the generalized formation free energy of the corresponding solid compound relative to bulk lead and molecular fluorine and chlorine. The experimental[31,32] and calculated data for ΔH_f are listed in Table I, showing that the calculated results are very consistent with the experimental results.

Figure 2 shows the calculated stability quadrangle for Pb-F-Cl systems in the μ_F, μ_{Cl} plane. The dashed zone represents the region of stability of PbFCl. Equations (5) and (6) determine the PbF_2-rich (line AD) and $PbCl_2$-rich (line BC) environments, respectively. The labels A, B, C, and D represent (F-rich and Cl-rich) limit, Cl-rich limit, F-poor limit, and Cl-poor limit, respectively.

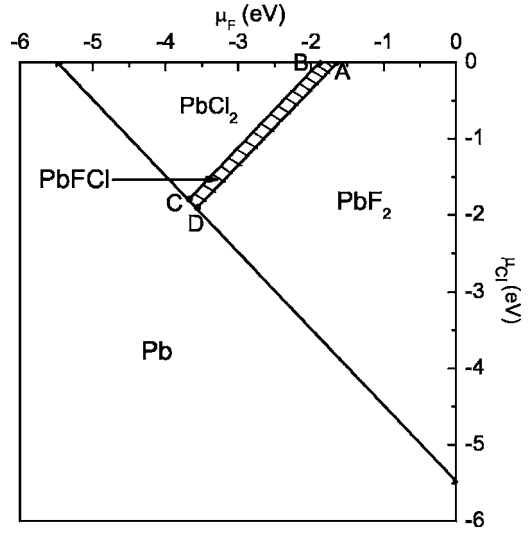

FIG. 2. The calculated stability quadrangle for Pb-F-Cl systems in the μ_F, μ_{Cl} plane. The dashed zone represents the region of stability of PbFCl. The lines AD and BC are determined by Eqs. (5) and (6), respectively.

III. RESULTS AND DISCUSSION

We first considered a variety of isolated neutral and charged intrinsic defects, including vacancies (V_{Pb}, V_F, and V_{Cl}) and interstitials (Pb_i, F_i, and Cl_i) for three elements, antisite defects F_{Cl} (F atom at Cl site), and Cl_F (Cl atom at F site). For the case of interstitials, the only stable position for the interstitial ions is near the center of the face of Pb-Cl and the interstitial ions may relax in the *c*-axis direction, which is similar to Islam's result. Then the formation energies for

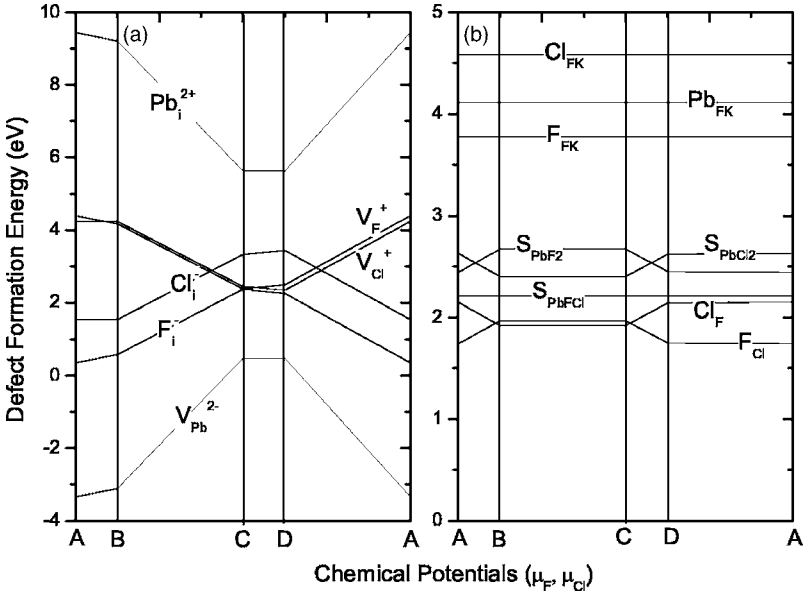

FIG. 3. Defect formation energies for charged defects (a) and antisite defects, Schottky defects, and Frenkel defects (b) in PbFCl as a function of the atomic chemical potentials. For charged defects (a), the Fermi energy is set as the middle in the band gap. The labels A, B, C, and D are defined in Fig. 2.

TABLE II. Defect formation energies (in eV) for charged vacancies, charged interstitials, and antisite defects. The chemical potentials are fixed to the values given by the A, B, C, and D point. The Fermi energy is set at the middle of the gap. The values reported by Islam are also listed for comparison.

Defect	A point F-rich and Cl-rich	B point Cl-rich	C point F-poor	D point Cl-poor	Islam's result
V_F^+	4.4	4.17	2.35	2.49	5.82
V_{Cl}^+	4.24	4.24	2.45	2.34	3.09
V_{Pb}^{2-}	−3.34	−3.11	0.47	0.47	19.77
F_i^-	0.35	0.58	2.40	2.26	−1.31
Cl_i^-	1.54	1.54	3.33	3.44	2.93
Pb_i^{2+}	9.44	9.21	5.63	5.63	−10.03
F_{Cl}	1.74	1.97	1.97	1.75	−1.69
Cl_F	2.15	1.92	1.92	2.14	3.74

three Frenkel pairs Pb_{FK}, F_{FK}, and Cl_{FK} and three Schottky defects $(V_{Pb}+V_F+V_{Cl})$, $(V_{Pb}+2V_F)$, $(V_{Pb}+2V_{Cl})$ were also calculated by putting the defect pair in the same supercell. For the Frenkel defect, the interstitial was initially located in the face of Pb-Cl, similar to the isolated interstitial, and the vacancy was selected near the interstitial. Several possible configurations of Frenkel defects were calculated. The lowest energies are considered as the formation energies.

The formation energies for isolated charged defects, antisite defects, Schottky defects, and Frenkel defects in PbFCl as a function of the atomic chemical potentials along the directions A→B→C→D→A are shown in Fig. 3. In Table II, the defect formation energies of isolated charged vacancies and interstitial defects and the antisite defects are listed for A, B, C, and D points, assuming that the Fermi energy level is located at the middle of the band gap. For comparison, the results reported by Islam.[18] using atomic simulation method with empirical interatomic potentials are also present. It is interesting to find that V_{Pb}^{2-} even has negative formation energies at anion-rich conditions. However, the negative formation energies do not mean that V_{Pb}^{2-} can be spontaneously formed, because some charge-compensating defects are expected to appear to maintain the charge neutrality in the whole system. These charge-compensating defects could be the defect pair, such as Schottky and Frenkel defects, which are the typical defects in ionic crystals.

The formation energies for V_F and V_{Cl} are close but still have a little difference under different chemical environments. In particular, V_F has lower formation energy than V_{Cl} and hence, should be more abundant in F-poor condition. While in Cl-poor condition, V_{Cl} should dominate. The formation energy for F_i^- is lower than that of Cl_i^- in the entire atomic chemical potential. This may be explained by the fact that the ionic radius of F^- (1.33 Å) is smaller than that of Cl^- (1.81 Å). Due to the larger ionic radius of Cl^-, a higher energy is required to relax the surrounding atoms, leading to a larger space to be occupied by the interstitial Cl^-. For the antisite defects of F_{Cl} and Cl_F, the formation energies are dependent on their chemical potentials. Under the F-poor (Cl-poor) condition, $Cl_F(F_{Cl})$ has the lower formation energy,

TABLE III. Formation energies (in eV) for Schottky and Frenkel defects and the sum of corresponding formation energies for neutral and charged isolated defects. The values in parentheses for Schottky and Frenkel defects are the cohesion energies. The chemical potentials for Schottky $(V_{Pb}+2V_F)$ and Schottky $(V_{Pb}+2V_{Cl})$ are fixed at line AD (PbF_2-rich) and BC ($PbCl_2$-rich), respectively, defined in Fig. 2. For comparison, the results of Islam are also shown.

Defect	This work	Results of Islam
Schottky $(V_{Pb}+V_F+V_{Cl})$	2.21 (2.95)	4.73
$V_{Pb}^0+V_F^0+V_{Cl}^0$	10.81	
$V_{Pb}^{2-}+V_F^++V_{Cl}^+$	5.16	
Schottky $(V_{Pb}+2V_F)$	2.63 (2.57)	5.27
$V_{Pb}^0+2V_F^0$	10.93	
$V_{Pb}^{2-}+2V_F^+$	5.20	
Schottky $(V_{Pb}+2V_{Cl})$	2.67 (2.68)	2.43
$V_{Pb}^0+2V_{Cl}^0$	10.65	
$V_{Pb}^{2-}+2V_{Cl}^+$	5.35	
Frenkel $(V_{Pb}+Pb_i)$	4.11 (1.23)	9.75
$V_{Pb}^0+Pb_i^0$	11.45	
$V_{Pb}^-+Pb_i^+$	7.87	
$V_{Pb}^{2-}+Pb_i^{2+}$	5.34	
Frenkel (V_F+F_i)	3.78 (1.11)	4.52
$V_F^0+F_i^0$	7.12	
$V_F^++F_i^-$	4.89	
Frenkel $(V_{Cl}+Cl_i)$	4.58 (1.37)	6.02
$V_{Cl}^0+Cl_i^0$	8.44	
$V_{Cl}^++Cl_i^-$	5.95	

indicating that the $Cl^-(F^-)$ is easier to occupy $F^-(Cl^-)$ site.

From Table II, it is found that the present results are very different from those reported by Islam. For example, Islam's formation energy for V_{Pb}^{2-} is about 20 eV higher than our calculated value. This distinct discrepancy mainly originates from the different reference energies adopted in the calculations. Islam's formation energy for an interstitial ion means the energy required to move the ion from infinity to the interior of crystal, and the formation energy for a vacancy is defined as the energy required to remove an ion from its interior site to infinity. However, in the present calculations, the reference energies are the chemical potentials of elemental solid (fcc Pb) and molecule (F_2 and Cl_2). In fact, this method is more practical and close to the real system.

The defect formation energies are also strongly dependent on the electron Fermi energy for the charge states, shown in Fig. 4. For each defect, only the charge state that gives the lowest formation energy with respect to the Fermi level is depicted. The solid dots denote the values of E_F where transition between charge states happens, and the corresponding value of E_F is the defect transition energy $\varepsilon_\alpha(q/q')$ defined

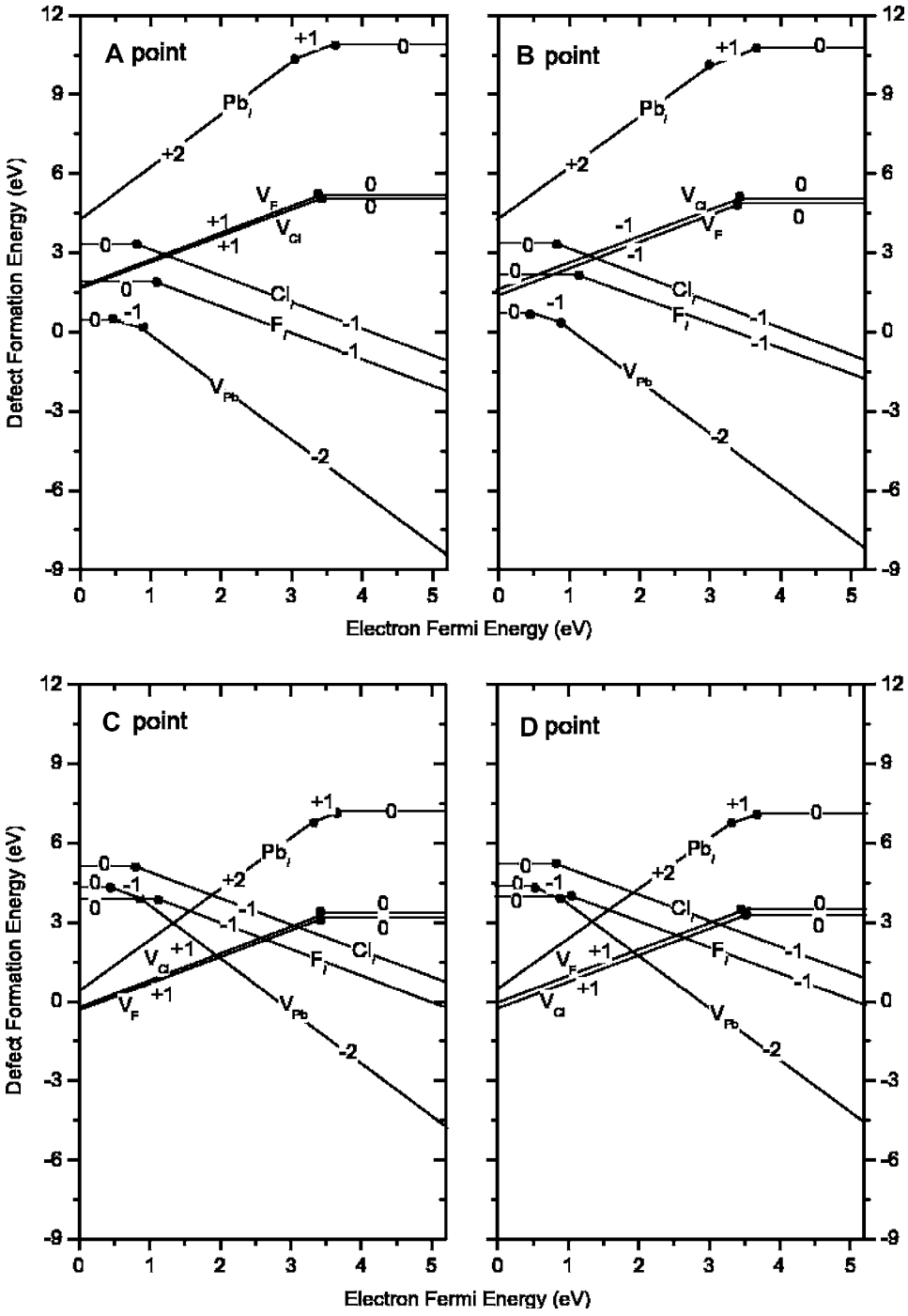

FIG. 4. Formation energies as a function of the electron Fermi energy E_F at atomic chemical potentials A, B, C, and D shown in Fig. 2. The signed numbers stand for the charge states of the defects. Solid dots denote the values of E_F where transition between charge states happens.

in Eq. (3). From Fig. 4, the stable states of the isolated defects are found to be charged in a wide range of the Fermi level, showing the strong ionic character in PbFCl crystals.

The possibility of formatting charge-compensating defect pairs is expected based on the charge-neutrality requirement. The dominant defect species can be determined by finding the smallest formation energy of the charge-neutral defect reaction. The interaction including Coulombic attraction and charge transfer between the defects with opposite charge states can significantly lower the formation energy. The formation energies of Frenkel and Schottky defects are shown in Fig. 3(b). To analyze the interaction between the defects forming Frenkel and Schottky defects, the formation energies for Schottky and Frenkel defects and the sum of corresponding formation energies for neutral and charged isolated defects are shown in Table III. The chemical potentials for Schottky ($V_{\mathrm{Pb}}+2V_{\mathrm{F}}$) and Schottky ($V_{\mathrm{Pb}}+2V_{\mathrm{Cl}}$) are fixed at line AD ($PbF_2$-rich) and BC ($PbCl_2$-rich), respectively, defined in Fig. 2. For comparison, the Islam's results are also shown. Our calculated results show that Schottky defects have much lower formation energies of 2.21, 2.63, and 2.67 eV for S_{PbFCl}, S_{PbF2}, and S_{PbCl2}, respectively, than those of Frenkel defects (4.11, 3.78, and 4.58 eV for Pb_{FK}, F_{FK}, and Cl_{FK}, respectively), thus expecting that the Schottky defects are dominant in PbFCl. In fact, the Schottky defects often happen in the ionic crystals which are composed of

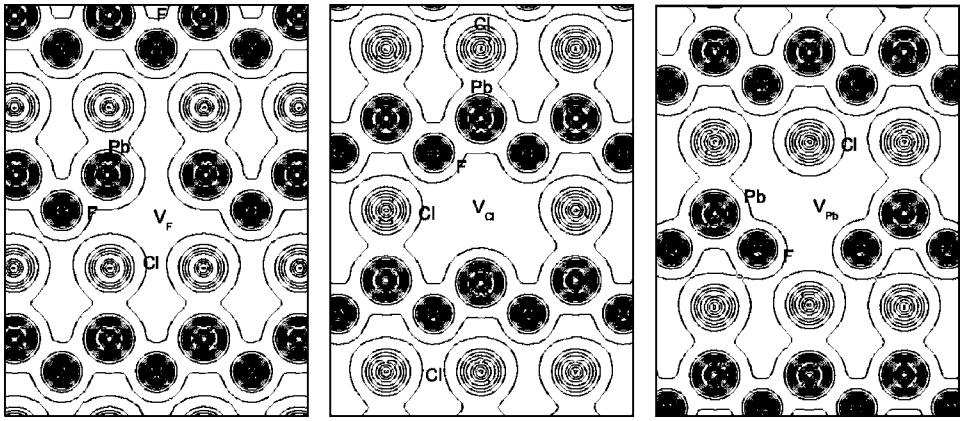

FIG. 5. Contour plot of calculated charge density of vacancy-containing PbFCl. The contour lines are from 0.07 to 11.3 e/Å^3 with an interval of 0.4 e/Å^3.

elements with close ionic radii. For example, the Schottky defects are also found to be dominant in PbF_2 and $PbCl_2$ crystals.[33] As shown in Fig. 3(b), Frenkel defects and Schottky ($V_{Pb}+V_F+V_{Cl}$) defects are independent on the chemical potentials since they are still stoichiometric. While for S_{PbF2} and S_{PbCl2} defects, the formation energies are dependent on the chemical potentials.

From Table III, it is also found that the sum of formation energies for the isolated defects significantly decrease with increasing charge states, suggesting that both Frenkel and Schottky defects have the tendency to be charged. This is reasonable because PbFCl is a typical ionic crystal with strong electronegativity for F and Cl ions. Furthermore, the contour plot of the calculated charge density of vacancy-containing PbFCl, shown in Fig. 5, exhibits strong ionic characteristics since the overlapped covalent contribution cannot be observed.

When isolated charged defects come close to each other, forming Frenkel or Schottky defects, the interaction between the individual charged defects can further lower their formation energies. This interaction can be described by the cohesive energy obtained from the sum of isolated charged formation energies minus the formation energy of Schottky or Frenkel defects. The present results show that the cohesive energies of Schottky defects are 1 eV higher than those of Frenkel defects, shown in Table III (values in parentheses), suggesting that Schottky defects could have lower energy states compared with the Frenkel defects. This may be one of the reasons why Schottky defects have lower formation energies. Additionally, our results indicate that S_{PbFCl} has the lowest formation energy, which is in accord with the previous experimental result showing that the Schottky defect with both types of anion is dominant.[34] In contrast, Islam's results show S_{PbCl2} has the lowest formation energy. It should be noticed that, in Islam's calculations, the formation energies for Schottky defects were obtained by considering the formation energies of isolated vacancies and the cohesive energy between them. Unfortunately, the cohesive energies in his calculations were difficult to be precisely determined; thus, the results were not very accurate. In the present calculations, the formation energies for Schottky defects were directly obtained by calculating the total energy of relaxed Schottky-defect-containing supercells, therefore providing more reliable results.

The formation of vacancies and interstitials can cause structural relaxations of the ions surrounding the defect. For

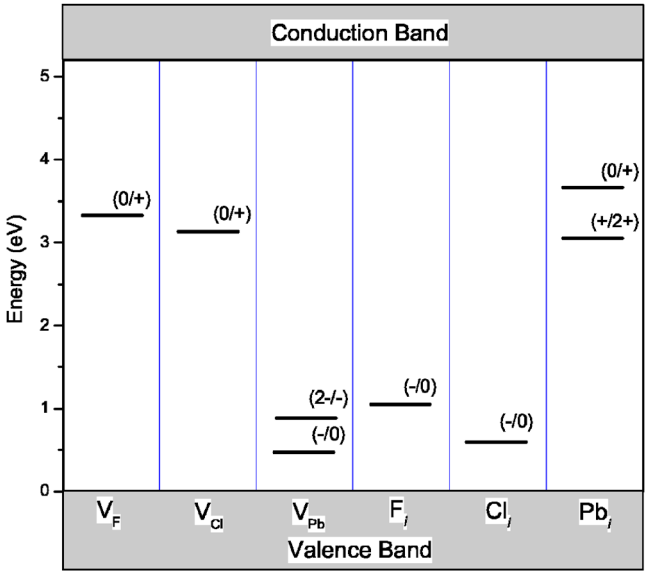

FIG. 6. (Color online) Calculated defect transition energy levels $\varepsilon_\alpha(q/q')$ according to Eq. (3).

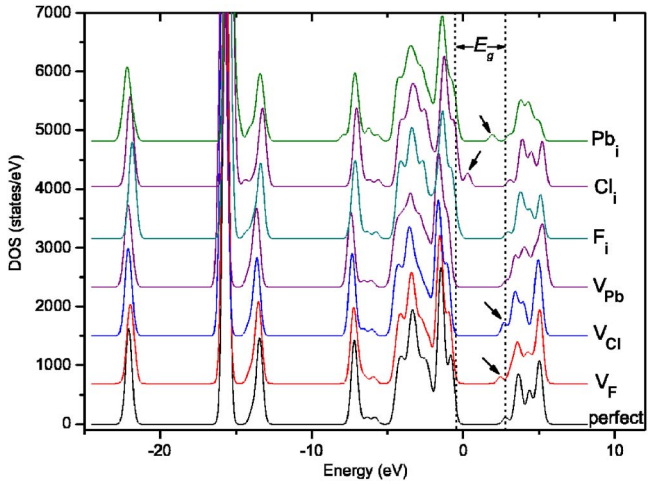

FIG. 7. (Color online) Densities of states for neutral perfect and defective PbFCl supercells. The arrows denote the extra levels in the band gap.

TABLE IV. Defect transition levels $\varepsilon_\alpha(q/q')$ of Eq. (3).

Level	V_{Pb}	V_F	V_{Cl}	Pb_i	F_i	Cl_i
(0/+)		$E_C-3.32$	$E_C-3.12$	$E_C-3.05$		
(+/2+)				$E_C-3.67$		
(−/0)	$E_V+0.47$				$E_V+1.05$	$E_V+0.57$
(2−/−)	$E_V+0.9$					

F vacancy, the nearest-neighboring F^- ion in the F^- ion plan exhibits inward relaxation by 0.79%, and the nearest-neighboring Pb^{2+} ion exhibits outward relaxation by 3.8% with a corresponding relaxation energy of 0.15 eV. For Cl vacancy, the nearest-neighboring Cl^- ion in the Cl^- ion plan shows inward relaxation by 2.8%, and the first near-neighboring Pb^{2+} ion exhibits outward relaxation by 2.1% with a corresponding relaxation energy of 0.20 eV. Such relaxations can be understood as follows. When an anion is removed, the electrostatic repulsive force for other anions disappeared, causing the neighboring anions to relax inward, whereas the electrostatic attractive force for the cations is also missing, causing the neighboring cations to relax outward.

The calculated defect transition energy levels are shown in Fig. 6 and are also listed in Table IV. It can be found that the donorlike defects induced by anion vacancies and cation interstitials have deeper levels than those induced by cation vacancies and anion interstitials. For instance, the calculated V_F level $E(0/+)=E_C-3.32$ eV and V_{Cl} level $E=E_C-3.12$ eV are considerably deeper than the F_i level $E(-/0)=E_V+1.05$ eV and Cl_i level $E(-/0)=E_V+0.57$ eV. In addition, the Pb_i also forms deeper levels than that of V_{Pb}. From the calculated results, there are several deep traps with energy of 1.53–2.15 eV for F, Cl vacancies, and Pb interstitials. These levels could act as electron traps or hole traps which are responsible for the thermoluminescence peaks. The energy levels of defects deduced from thermoluminescence measurements[35,36] are in the range of 0.3–1.2 eV. However, the calculated trap levels cannot be definitely assigned to the thermoluminescence trap levels since the experimental levels may be also related to the impurity defects such as oxygen and hydroxyl. Therefore, other measurements, such as electron spin resonance and deep-level transient spectroscopy, are necessary for revealing the nature of experimental trap levels.

The total densities of states (DOS) profiles for the neutral perfect and defective PbFCl supercell are present in Fig. 7. The defective DOS profiles are similar to those of perfect the one, expect for some extra levels in the band gap. From our previous results,[13] the valence band maximum (VBM) is mainly composed of Cl $3p$ states, and Pb $6p$ states are the main component of the conduction band maximum (CBM). In the case of V_F and V_{Cl}, the highest occupied levels with one electron are located at 2.5 and 2.7 eV, respectively, which are composed of Pb $6p$ states near the vacancy and are donorlike levels at the vicinity of the VBM. V_{Pb} does not induce evident extra states in the gap because the F $2s$ component in the CBM is rather little compared with Pb $6p$ states. For the case of Pb_i, the extra states appear at 2.0 eV, which is composed of the $6p$ states of interstitial Pb ions. Cl_i also forms the extra states located at 0.3 eV, which can be understood by the fact that VBM is composed of Cl $3p$ states. There are no evident extra states in the gap for the F_i case because the F $2p$ component in VBM is small.

IV. SUMMARY

We have performed first-principles pseudopotential calculations for the intrinsic defects in PbFCl. The main results can be summarized as follows:

(1) The defect formation energies for various isolated charged states are calculated with a function of atomic chemical potentials and electron chemical potentials. In a wide range of electron chemical potential, the full ionized states of defects are stable, suggesting that there is a strong tendency toward ionization of the defects. The formation energies of Schottky are much lower than those of Frenkel defects, indicating that the Schottky defects are energetically favorable and dominant. The Schottky defect S_{PbFCl} has the lowest formation energy of 2.21 eV. The calculated results are in accord with the experiment.

(2) Defect transition energy levels occur between different charged states. The anion interstitials and cation vacancy form acceptorlike defects with transition energies of 1.05, 0.57, and (0.47, 0.9) eV for F_i, Cl_i, and V_{Pb}, respectively. While V_F, V_{Cl} and Pb_i have high transition energies of more than 3 eV.

(3) There are evident extra states located in the band gap for Pb_i, Cl_i, V_{Cl}, and V_F observed from the profiles of densities of states for defective supercells.

ACKNOWLEDGMENTS

This work was supported by National Natural Science Fund of China (No. 10404028) and the Ministry of Science and Technology of China (863 program, Grant No. 2002 AA 324070). We thank B.C. Pan for helpful discussions.

*Corresponding author. Email address: lbo@ustc.edu.cn

[1] F. Hulliger, *Structure Chemistry of Layer-Type Phases* (Dordrecht, Reidel, 1975).
[2] T. K. Anh, L. Q. Minh, W. Strek, and C. Barthou, J. Lumin. **72-74**, 745 (1997).
[3] M. Secu, L. Matei, T. Serban, E. Apostol, Gh. Aldica, and C. Silion, Opt. Mater. **15**, 115 (2000).
[4] Y. R. Shen, T. Gregorian, and W. B. Holzapel, High Press. Res. **7**, 73 (1991).
[5] F. Decremps, M. Fischer, A. Polian, J. P. Itie, and M. Sieskind, Phys. Rev. B **59**, 4011 (1999).
[6] Jianming Chen, Dingzhong Shen, R. Mao, G. Ren, and Z. Yin, J. Cryst. Growth **250**, 393 (2003).
[7] J. Chen, D. Shen, H. Zhang, H. Shi, and Z. Yin, J. Cryst. Growth **263**, 431 (2004).
[8] J. Chen, D. Shen, G. Ren, R. Mao, and Z. Yin, J. Phys. D **37**, 938 (2004).
[9] A. J. H. Eijkelenkamp, J. Solid State Chem. **19**, 313 (1976).
[10] A. J. H. Eijkelenkamp, Solid State Commun. **18**, 295 (1976).
[11] V. Kanchana, G. Vaitheeswaran, and M. Rajagopalan, J. Phys. Condens. Matter **15**, 1677 (2003).
[12] F. E. H. Hassan, H. Akbarzadeh, S. J. Hashemifar, and A. Mokhtari, J. Phys. Chem. Solids **65**, 1871 (2004).
[13] B. Liu, C. Shi, M. Yin, Y. Fu, and D. Shen, J. Phys. Condens. Matter **17**, 5087 (2005).
[14] A. F. Halff and J. Schoonman, J. Solid State Chem. **27**, 397 (1979).
[15] J. Shoonman, A. F. Halff, and G. Blasse, Solid State Commun. **13**, 677 (1973).
[16] J. Schoonman, G. J. Dirksen, and G. Blasse, J. Solid State Chem. **7**, 245 (1973).
[17] M. S. Islam, Philos. Mag. A **64**, 1119 (1991).
[18] M. S. Islam, J. Solid State Chem. **85**, 251 (1990).
[19] X. Gonze, J.-M. Beuken, R. Caracas, F. Detraux, M. Fuchs, G.-M. Rignanese, L. Sindic, M. Verstraete, G. Zerah, F. Jollet, M. Torrent, A. Roy, M. Mikami, P. Ghosez, J.-Y. Raty, and D. C. Allan, Comput. Mater. Sci. **25**, 478 (2002).
[20] The ABINIT code is a common project of the Université Catholique de Louvain, Corning, Inc., and other contributors (URL http://www.abinit.org).
[21] S. Goedecker, SIAM J. Sci. Comput. (USA) **18**, 1605 (1997).
[22] M. C. Payne, M. P. Teter, D. C. Allan, T. A. Arias, and J. D. Joannopoulos, Rev. Mod. Phys. **64**, 1045 (1992).
[23] X. Gonze, Phys. Rev. B **54**, 4383 (1996).
[24] J. P. Perdew, K. Burke, and M. Ernzerhof, Phys. Rev. Lett. **77**, 3865 (1996).
[25] W. Kohn and L. J. Sham, Phys. Rev. **140**, A1133 (1965).
[26] M. Fuchs and M. Scheffler, Comput. Phys. Commun. **119**, 67 (1999).
[27] W. H. Press, B. P. Flannery, S. A. Teukolsky, and W. T. Vetterling, *Numerical Recipes, The Art of Scientific Computing*, FORTRAN Vers. (Cambridge University Press, Cambridge, MA,1989).
[28] S. B. Zhang and J. E. Northrup, Phys. Rev. Lett. **67**, 2339 (1991).
[29] D. B. Laks, C. G. Van de Walle, G. F. Neumark, P. E. Blöchl, and S. T. Pantelides, Phys. Rev. B **45**, 10965 (1992).
[30] S. B. Zhang, S. H. Wei, A. Zunger, and H. Katayama-Yoshida, Phys. Rev. B **57**, 9642 (1998).
[31] *NIST Chemistry WebBook, NIST Standard Reference Database No. 69*, edited by W. G. Mallard and P. J. Linstrom (National Institute of Standards and Technology, Gaithersburg, MD, 2005).
[32] *LANGE's Handbook of Chemistry*, 15th ed., edited by John A. Dean (McGraw-Hill, Inc., New York, 1999), Sec. 6, p. 6.98.
[33] V. G. Plekhanov, Prog. Mater. Sci. **49**, 787 (2004).
[34] A. F. Halff and J. Schoonman, J. Solid State Chem. **27**, 397 (1979).
[35] B. Liu, C. Shi, J. Chen, and D. Shen, IEEE Trans. Nucl. Sci. **52**, 527 (2005).
[36] K. Somaiah and S. R. Moinuddin, J. Mater. Sci. Lett. **6**, 417 (1987).